Medicine in Drug Discovery 23 (2024) 100194

Contents lists available at ScienceDirect

Medicine in Drug Discovery

journal homepage: www.elsevier.com/locate/medid

Repurposing nitrofurantoin as a stimulant of fibroblast extracellular matrix repair for the treatment of emphysema

Mathew N. Leslie [a,b], Zara Sheikh [a,c], Dikaia Xenaki [d], Brian G. Oliver [d,e], Paul M. Young [a,f], Daniela Traini [a,b], Hui Xin Ong [a,b,*]

[a] Respiratory Technology, The Woolcock Institute of Medical Research, Sydney, NSW 2113, Australia
[b] Faculty of Medicine, Healthy and Human Sciences, Macquarie University, Sydney, NSW 2109, Australia
[c] School of Pharmacy, Brac University, Dhaka 1212, Bangladesh
[d] Respiratory Cellular and Molecular Biology, Woolcock Institute of Medical Research, Sydney, NSW 2113, Australia
[e] School of Life Sciences, University of Technology Sydney, Sydney, NSW 2007, Australia
[f] Department of Marketing, Macquarie Business School, Macquarie University, Sydney, NSW 2109, Australia

ARTICLE INFO

Keywords:
Emphysema
Nitrofurantoin
Fibroblast
Extracellular matrix
Pulmonary fibrosis
Lung

ABSTRACT

Emphysema is a respiratory disease that causes the progressive loss of lung extracellular matrix (ECM) organisation, subsequently undermining lung integrity and reducing lung function. Fibroblasts must constantly repair damage to the lungs to preserve lung health, however, fibroblast ECM repair is reduced during emphysema, causing ECM damage to outweigh fibroblast ECM maintenance. Current treatments for emphysema fail to address the root causes of emphysematous progression, highlighting the need for novel methods of treating emphysema. Nitrofurantoin is a broad-spectrum antibiotic indicated for the treatment of urinary tract infections that also displays potential as a novel avenue of emphysema treatment. Nitrofurantoin is known to potentially cause fibrotic effects that could be repurposed to increase fibroblast repair and outweigh the progressive ECM damage of the emphysematous lung. Therefore, this study examined the effects of nitrofurantoin treatment on primary human lung fibroblasts derived from emphysema patients to determine if the drug holds potential as a novel treatment for emphysema. Nitrofurantoin was shown to stimulate migration and alter fibroblast morphology by increasing cell area and reducing roundness, suggesting that it could induce an ECM-repair primed phenotype in fibroblasts. Interestingly, nitrofurantoin treatment did not alter collagen-IV, perlecan, periostin or tenascin-C deposition, though fibronectin deposition was significantly upregulated at a higher dosage (20 μg/mL). This study highlighted the nitrofurantoin induced changes to fibroblast motility and morphology that facilitate ECM repair. Thus, nitrofurantoin induced pulmonary fibrosis could be caused by a change in cell phenotype that subsequently upregulates ECM repair, indicating its potential as a treatment for emphysema.

1. Introduction

Fibroblasts are cells that reside within the lung parenchyma and work to maintain the integrity of the extracellular matrix (ECM), a dynamic network of fibrous proteins and proteoglycans that structurally supports cells and governs the mechanical properties of the lung, including stiffness and lung elasticity [1–5]. Fibroblasts work to repair damage to the lung caused by the introduction of irritants, by lung injuries or by the gradual wear caused during the cyclic stretch of breathing [6,7]. Fibroblast ECM maintenance is of critical importance to lung health, as a shift in the lung mechanical environment can have wide-reaching effects on the behaviour of mechanosensitive cells populations, cells that detect mechanical forces and alter cellular behaviour in response. Fibroblasts, among many other lung cell populations, are known to be mechanosensitive and drastically alter their behaviour due to a change in substrate stiffness or other forces [8–12].

Emphysema is characterised by severe alterations to the lung environment reflected by the progressive destruction of the lung ECM and loss of alveolar walls [3,13–15]. The emphysematous lung is known to have decreased parenchymal stiffness and experience diminished stretch forces when breathing due to lung hyperinflation, the inability to fully retract the lung during exhalation. This pathological hyperinflation

* Corresponding author.
E-mail address: huixin.ong@mq.edu.au (H.X. Ong).

https://doi.org/10.1016/j.medidd.2024.100194
Received 11 February 2024; Received in revised form 24 May 2024; Accepted 17 June 2024
Available online 22 June 2024

causes reduced gas exchange and disrupts the stretch forces, therefore distorting crucial regulatory mechanical cues experienced by fibroblasts in the emphysematous lung [16]. Furthermore, fibroblasts rely upon the regulatory cues provided by fibroblast-ECM protein interactions to guide ECM repair, yet the altered composition of the emphysematous lung likewise disturbs this form of regulation. The insufficient ECM maintenance performed by emphysematous fibroblasts is likely a result of cellular dysregulation due to altered biomechanical cues, such as reduced stretch forces, decreased lung stiffness, and altered ECM composition [17,18]. Our recent study has suggested that the emphysematous lung environment may induce a fibroblast phenotype that is unsuited to ECM repair through pathological adaptation in lung fibroblasts, disrupting the ability of emphysematous fibroblasts to correctly respond to lung regulatory cues. However, an increase in fibroblast ECM repair could reverse these pathological changes and may sufficiently increase fibroblast ECM deposition to halt emphysematous progression, restoring the regulatory cues of the healthy lung.

The antibiotic nitrofurantoin is recommended as a first line therapy for urinary tract infections [19]; however, it has been known to potentially cause adverse effects such as pulmonary fibrosis [20,21]. Despite the adverse effects, nitrofurantoin is an approved therapy by the Food and Drug Administration FDA-(FDA Reference ID: 3368447). Raised lung ECM stiffness, due to nitrofurantoin-induced pulmonary fibrosis, could cause a further upregulation of fibroblast-mediated ECM maintenance due to the mechanosensitivity of fibroblasts. Furthermore, this increased fibroblast ECM repair is more likely to create a recursive loop of rising ECM stiffness and rising fibroblast activity that may overcome the progressive ECM damage of emphysema. Stimulation of ECM deposition through fibrosis represents a novel avenue of treatment for emphysema that could potentially address a major underlying cause of emphysema, rather than merely addressing symptoms, as done by current steroid and anti-inflammatory treatments [22]. Therefore, the present study aims to explore the effect of nitrofurantoin on fibroblasts and determine if the treatment can improve the dysfunctional ECM repair of emphysematous fibroblasts. The viability and potential of nitrofurantoin as a treatment for emphysema was investigated by assessing nitrofurantoin cellular toxicity and the influence of the drug on emphysematous fibroblast dynamic cellular behaviour. A range of emphysematous fibroblast processes relating to ECM maintenance, including cytokine expression (IL-6 and IL-8), cellular motility, morphology, and ECM protein deposition were analysed to determine changes caused by nitrofurantoin treatment.

2. Materials and methods

2.1. Primary cell isolation

Primary human lung fibroblasts (PHLF) were extracted from the explanted or resected lung parenchyma of emphysema patients following resection or lung transplantation. Written informed consent was obtained from each patient pre-operatively and the study was approved by a human research ethics committee (approval code #X14-0045). A segment of parenchymal tissue (1 cm^3) was taken from the discarded lung of each patient and divided into small pieces (1 mm^3). These smaller pieces of parenchymal tissue were washed with Hank's buffered salt solution (HBSS) and a minimum of ten washed pieces of parenchymal tissue were seeded in 75 cm^2 cell culture flasks (Corning Costar, Massachusetts, USA). The tissue segments were maintained in Dulbecco's Modified Eagle Medium (DMEM; Sigma-Aldrich, Sydney, Australia) supplemented with 5 % FBS (*v/v*) (FBS; Invitrogen, Melbourne, Australia) and 1 % antibiotic antimycotic solution (Sigma-Aldrich) at 37 °C and 5 % CO_2. After 2–4 weeks, the cells reached confluency and were identified as fibroblasts by observing the growth patterns and cellular morphology before being passaged. PHLF were then cultured in DMEM – low glucose (Sigma-Aldrich) supplemented with 10 % FBS (*v/v*; Invitrogen), 2 % (*v/v*) HEPES solution, 1 % (*v/v*) L-glutamine solution (Gibco, Invitrogen, Melbourne, Australia) and 1 % antibiotic antimycotic solution (*v/v*; Sigma-Aldrich). All experiments on PHLF were performed between passages 2 and 6.

Additionally, PHLF were treated with the drug nitrofurantoin (Merck-Millipore, Massachusetts, USA) at 2, 10 or 20 μg/mL 24 h after seeding (standard treatment group) or 48 h after seeding (delayed treatment group). Pulmonary fibrosis is an uncommon adverse effect of nitrofurantoin treatment; therefore, a higher dose could be necessary to induce the desired fibroblast ECM deposition. Thus, 20 μg/mL was chosen as the maximum possible nitrofurantoin concentration (dose) that could induce ECM deposition without greatly reducing fibroblast viability (Fig. 2). Additionally, the concentrations 2 and 10 μg/mL were examined to provide an understanding of the effect of nitrofurantoin concentrations that did not negatively impact cell viability on fibroblasts and to determine if the impact of nitrofurantoin was dose dependent. Nitrofurantoin treatments were prepared by dissolving raw nitrofurantoin in DMSO then diluting to the desired concentration using cell culture media while ensuring that the final concentration of DMSO in solution was below 1 % (*v/v*).

2.2. Cell culture

The healthy human lung fibroblast cell line, WI-38 (Code: 90020107) were purchased from CellBank Australia (CBA, Westmead, NSW, Australia) and maintained in minimum essential medium eagle (MEME; Sigma-Aldritch) supplemented with 10 % (*v/v*) FBS (Invitrogen), and 1 % (*v/v*) sodium pyruvate (Gibco). All experiments on WI-38 were performed between 22 and 40 population doublings.

All cell culture was performed in 6, 48 or 96 well plates (Corning Costar) coated with collagen type-I from rat tail (10 μg/cm^2; Sigma-Aldrich) and all cells were treated with 2 ng/mL of TNF-α (InVitro Technologies, Melbourne, Australia) or 2 ng/mL of TGF-β (BioLegend, California, USA).

2.3. MTS assay

Cell viability was assessed using an MTS assay (CellTitre 96® Aqueous One Solution Cell Proliferation Assay, Promega, Sydney, NSW, Australia), a colorimetric method that detects the reduction of 3-(4,5-dimethylthiazol-2-yl)-5-(3-carboxymethoxyphenyl)-2-(4-sulphophenyl)–2H-tetrazolium inner salt (MTS) by mitochondrial dehydrogenase in living cells. All MTS assays were conducted according to the manufacturer's protocols. Fibroblasts were seeded at a density of $4x10^3/cm^2$ in 96-well plates and subsequently treated with nitrofurantoin for 24 h post seeding. Nitrofurantoin treatments were prepared by first dissolving the drug in 100 % (*v/v*) DMSO and then serially diluting to the desired nitrofurantoin concentration (3.5 to 600 μg/mL) using whole cell culture media. The cells were treated with nitrofurantoin for 72 h then washed using PBS before MTS reagent was applied to each well for 2 h. The absorbance of each well was measured at 490 nm using a SpectraMax M5 spectrophotometer (Molecular Devices LLC, San Jose, California) and compared against the absorbance value of cells treated with a vehicle control to determine the percentage cell viability of each treatment group. Nitrofurantoin treatments contained a maximum of 1 % DMSO to avoid DMSO cytotoxicity negatively impacting cell viability. A vehicle control was prepared alongside a control group to validate that DMSO did not cause cytotoxicity. A lower cell density was necessary for the MTS assay compared to the ELISA and ECM ELISA assays to ensure that the absorbance of each well remained within the range of detection.

2.4. Live-cell microscopy

A Nikon Eclipse Ti inverted microscope (Nikon, Tokyo, Japan) was used to acquire time-lapses of PHLF after treatment with nitrofurantoin. The microscope was equipped with an S Plan Fluor ELWD 10X Ph2 ADM

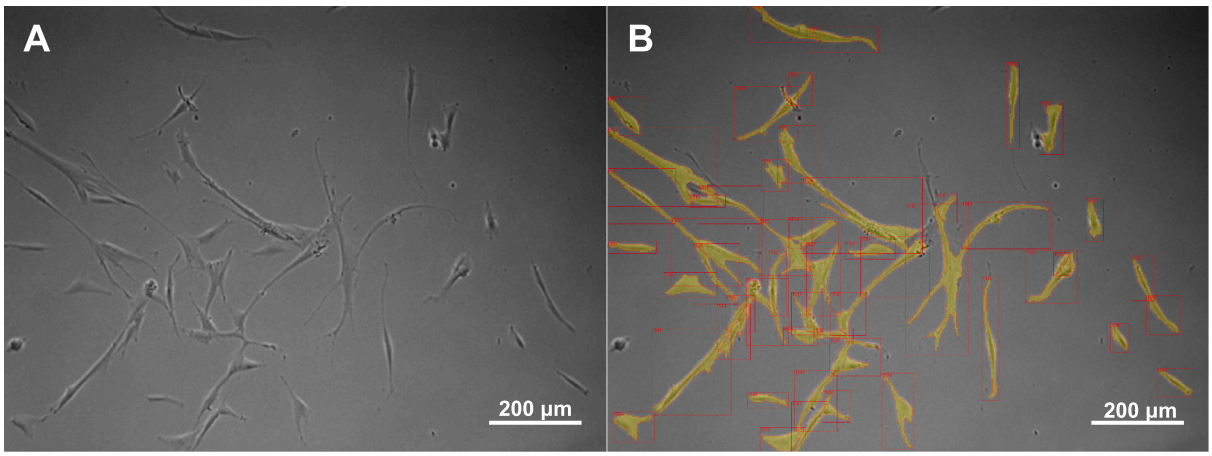

Fig. 1. An image of WI-38 fibroblasts (**A**) before and (**B**) after the application of the fibroblast detection model.

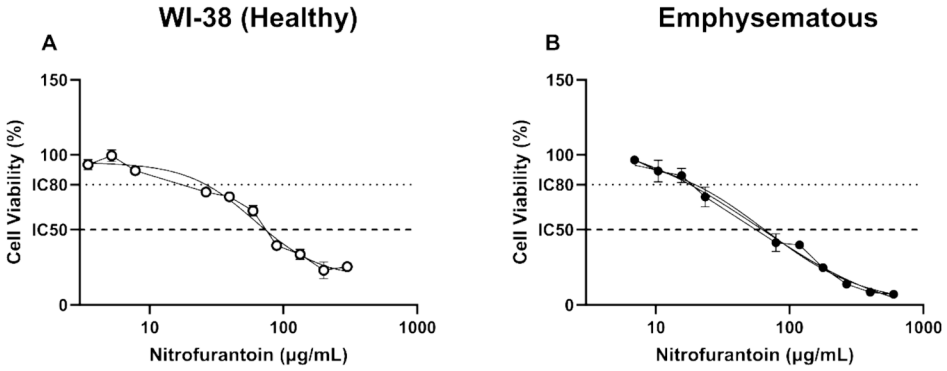

Fig. 2. Dose-response curves of (**A**) healthy (WI-38 cells) and (**B**) emphysematous primary fibroblasts after being treated with varying concentrations of nitrofurantoin for 72 h and examined by MTS assay. Absorbance values of untreated control cells were normalised to a 100 % value of fibroblast cell viability when treated with only a 1 % DMSO vehicle control. Dose-response curves were analysed by non-linear regression to fit a curve to the data and calculate the IC50 and IC80 of nitrofurantoin for healthy and emphysematous fibroblasts. (**A**) Nitrofurantoin was found to have an IC50 of 78.1 ± 1.7 µg/mL and an IC80 of 22.5 ± 3.0 µg/mL when applied to WI-38 fibroblasts. (**B**) Nitrofurantoin was found to have an IC50 of 64.8 ± 0.4 µg/mL and an IC80 of 19.6 ± 1.6 µg/mL when applied to primary emphysematous fibroblasts. Data is displayed as mean ± SEM, $n = 3$.

objective (Nikon, Tokyo, Japan), CoolSnap ES2 camera, CO_2 controller and TCH 882-G-COM Controller (Clear State Solutions, Melbourne, Victoria, Australia). Cells were seeded in 48 well plates (Corning Costar) at a density of 3.5×10^3 cells/cm^2 and treated with 2, 10 or 20 µg/mL of nitrofurantoin 24 h after seeding (standard treatment group) or 48 h after seeding (delayed treatment group). A time-lapse was captured through phase contrast microscopy by acquiring images in 15-minute intervals across a 24-hour time-period. Fibroblasts were incubated at 37 °C and 5 % CO_2 throughout the time-lapse acquisition. A deep learning model was trained using data gathered in these time-lapses to identify fibroblasts (Fig. 1) through the 'human-in-the-loop' training method using Cellpose [23,24], an open-source machine learning program. The resulting fibroblast detection model was then used with the ImageJ plugin, LIMTracker [25], to detect and track fibroblasts throughout the time-lapse then to generate data on cell morphology and migration. The fibroblast detection model was developed from 40 images each containing approximately 20 regions of interest (ROIs; 800 total). These ROIs were used to generate masks and then analysed using a batch size of 1 with 500 epochs to train the fibroblast detection model. A minimum of $n > 50$ cells were tracked for each treatment group with cells that were detected for less than 10 consecutive frames or cells that were less than below 1500 um^2 being excluded from analysis to eliminate erroneous fibroblast detection.

Fibroblast cell shape was analysed to determine roundness using the formula:

$$R = \frac{4 \times Area}{\pi \times MajorAxis^2}$$

This formula produces a number between 0 and 1, where 0 represents a highly non-circular shape and 1 represents a perfect circle.

2.5. Assessment of cytokine concentrations using ELISA

PHLF and WI-38 cells were seeded in 6-well plates (Corning Costar) at a density of 2.7×10^4 cells/cm^2 and subsequently treated with 2, 10 or 20 µg/mL of nitrofurantoin 24 h post seeding (termed as standard treatment group) or 48 h post seeding (delayed treatment group). Supernatant was collected from all treatment groups 96 h after seeding (72 h or 48 h post treatment) and the concentrations of interleukin-6 (IL-6) and interleukin (IL-8) were determined using enzyme-linked immunosorbent assay (ELISA) kits (BD OptEIA, BD Biosciences, Franklin Lakes, New Jersey, USA) according to the manufacturer instructions.

2.6. ECM ELISA

PHLF and WI-38 cells were seeded in 96-well plates (Corning Costar) at a density of 2.7 x 10^4 cells/cm^2 and then treated with 2, 10 or 20 µg/mL of nitrofurantoin 24 h after seeding (standard treatment group) or 48 h after seeding (delayed treatment group). The fibroblasts were washed with phosphate buffered saline (PBS) 96 h after seeding and

further treated with 16 mM NH_4OH for 30 mins to remove all fibroblasts while preserving the adherent ECM produced by the fibroblasts. The decellularised ECM underwent further PBS washing and was blocked with 0.1 % bovine serum albumin (BSA; *w/v*; Sigma-Aldrich) to prevent non-specific binding. The blocked ECM was then treated with the following antibodies for 2 h: monoclonal mouse anti-collagen-IV primary antibody (diluted 1:1000; Sigma-Aldrich), monoclonal mouse anti-fibronectin primary antibody (diluted 1:4000; Invitrogen), monoclonal mouse anti-periostin primary antibody (diluted 1:2000, BD Biosciences), monoclonal mouse anti-perlecan primary antibody (diluted 1:2000; Invitrogen), monoclonal mouse anti-tenascin-C (diluted 1:10000; Sigma-Aldrich) and mouse IgG isotype (diluted 1:1000, BD Biosciences). The ECM was then treated with an HRP-linked anti-mouse secondary antibody (diluted 1:2000; Cell Signaling Technology, Danvers, Massachusetts, USA) followed by TMB substrate (Thermofisher, Sydney, NSW, Australia). Additionally, ECM was treated with mouse IgG isotype to test for false positive results. Finally, 1 M H_3PO_4 was applied to each well to halt the reaction and the absorbance of each well was measured using a SpectraMax M2 plate reader (Molecular Devices) at 450 nm, with plate correction at 570 nm. Expression of each ECM protein (collagen-IV, fibronectin, periostin, perlecan and Tenascin-C) was determined by comparing absorbance of each treatment group against the untreated control group for each cell line.

2.7. Statistical analysis

All results are presented as the mean ± the standard error of the mean (SEM) of three biological replicates for WI-38 results and five biological replicates ($n = 5$) for PHLF results. Statistical significance was determined using the software GraphPad Prism (version 8.2.1, San Diego, California, USA) via one-way ANOVA with Tukey's multiple comparison post-test or student's unpaired *t*-test with a threshold of significance of $p < 0.05$.

3. Results & discussion

The drug nitrofurantoin could have potential as a novel avenue of treatment for emphysema by repurposing the drug's pulmonary fibrosis adverse effect to counteract the loss of lung ECM during emphysematous progression. Nitrofurantoin was primarily chosen for this study due to its fibrotic adverse effect, however, the antibiotic nature of the drug could also assist in treating respiratory infections, a frequent yet serious complication of emphysema [13,26]. This study examined the effects of nitrofurantoin treatment on primary human lung fibroblasts derived from emphysema patients to determine the potential of this drug as a novel form of treatment for emphysema. Nitrofurantoin cellular toxicity and the influence of the drug on emphysematous fibroblast cellular processes relating to ECM maintenance, including cytokine expression (IL-6 and IL-8), cellular motility, morphology, and ECM protein deposition were investigated to determine any changes induced by nitrofurantoin.

All fibroblasts in this study were seeded on cell culture plastic that had been coated with collagen-1 (10 μg/cm^2; Sigma-Aldrich) to improve cell adherence and better replicate the ECM of the lung parenchyma [27]. Furthermore, fibroblasts were treated with both 2 ng/mL of TNF-α (InVitro Technologies) and 2 ng/mL of TGF-β (BioLegend) in all studies to stimulate ECM protein deposition and to simulate aspects of the emphysematous lung inflammatory environment [28–31]. A high seeding density was used in the ELISA and ECM ELISA assays to present sufficient ECM deposition to be within the range of analysis of ECM ELISA.

3.1. Nitrofurantoin toxicity

3.1.1. MTS assay

The toxicity of nitrofurantoin on healthy and emphysematous fibroblasts was first assessed using an MTS assay (Fig. 2). Both healthy and emphysematous fibroblasts were treated with nitrofurantoin across a broad range of concentrations 24 h after seeding, and MTS reagent was added for a further 72 h to assess changes in cell viability 24 h post drug treatment. The vehicle control used in this experiment was not found to lower cell viability in comparison to untreated fibroblasts (data not shown). The range of concentrations examined by MTS was limited by the poor aqueous solubility of the drug (0.079 mg/mL at room temperature [32]). As a result, WI-38 fibroblasts were treated with nitrofurantoin concentrations ranging from 3.4 μg/mL to 300 μg/mL (Fig. 2A). Emphysematous fibroblasts were treated with nitrofurantoin concentrations ranging from 6.9 μg/mL to 600 μg/mL (Fig. 2B). The IC50 and IC80 were calculated by fitting a sigmoidal curve through non-linear regression. Nitrofurantoin was found to have an IC50 of 78.1 ± 2.9 μg/mL and an IC80 of 22.5 ± 5.2 μg/mL when applied to WI-38 fibroblasts (Fig. 2A), and an IC50 of 64.8 ± 0.6 μg/mL and an IC80 of 19.6 ± 2.3 μg/mL in case of primary emphysematous fibroblasts (Fig. 2B). These results are similar to previous research by Michiels et al, that determined the IC50 of WI-38 cells treated with nitrofurantoin to be 12.1 μg/mL [33]. The difference in IC50 results is most likely due to differences in nitrofurantoin incubation time or WI-38 confluency as the Michiels et al. study measured cell viability after 5 days of nitrofurantoin exposure, whereas this study measured cell viability after only 3 days post treatment.

Notably, the emphysematous fibroblast nitrofurantoin dose–response curve (Fig. 2B) had a lower Hill slope value (−1.16 ± 0.1) than that of the healthy fibroblasts in (Fig. 2A; −1.12 ± 0.1), yet cell viability of the diseased primary fibroblasts was reduced at lower nitrofurantoin concentrations than healthy fibroblasts. A significant difference in IC50 values was observed between WI-38 and emphysematous fibroblast cells (78.1 ± 1.7 μg/mL and 64.8 ± 0.4 μg/mL respectively, Table 1), suggesting that the PHLF were more sensitive to nitrofurantoin toxicity than the healthy fibroblasts, however, the absolute difference in IC50 of the healthy and PHLF cells remains similar. Furthermore, no significant differences in IC80 values were found between WI-38 and emphysematous fibroblast cells (Table 1). The 3 concentrations/doses chosen for this study, 2, 10 and 20 μg/mL, were selected based on the IC80 values of the two cell groups. Notably, nitrofurantoin cytotoxicity has previously been reduced through pharmaceutical formulation techniques such as spray drying [34] and would most likely also be reduced by nanoparticle-based formulations or polymeric drug delivery systems.

3.1.2. ELISA

The pro-inflammatory cytokine IL-6 and pleiotropic cytokine IL-8 were quantified using ELISA to examine the cytokine release profile of nitrofurantoin treated fibroblasts, as both emphysema and drug induced pulmonary fibrosis are closely linked to inflammation and irritation within the lung [35]. These specific cytokines were chosen for analysis due to the central roles they play in the inflammatory response. IL-6 is primarily pro-inflammatory and highly important to biological processes related to emphysematous progression, such as chronic inflammation, wound healing, the initiation of inflammatory responses and immune recruitment [36–39]. Similarly, IL-8 is another major mediator of inflammatory responses and displays both pro and anti-inflammatory activity. Additionally, IL-8 is involved in the immune response by acting

Table 1
Comparison of IC50, IC80 and Hill slope values for the nitrofurantoin dose–response curves of healthy and emphysematous fibroblasts. (Unpaired Student *t*-test, Mean ± SEM, $n = 3$, * $p < 0.05$).

	Healthy (WI-38)	Emphysematous Fibroblasts (PHLF)	*p* value
IC50 (μg/mL)	78.1 ± 1.7	64.8 ± 0.4	0.012*
IC80 (μg/mL)	22.5 ± 3.0	19.6 ± 1.6	0.730
Hill slope	−1.12 ± 0.1	−1.16 ± 0.1	0.458

as a neutrophil chemotactic agent and encourages neutrophil infiltration [26,40,41]. IL-6 and IL-8 expression provides an understanding of the lung fibroblasts inflammatory response induced by nitrofurantoin treatment. Fibroblasts were treated with 2, 10 or 20 μg/mL of nitrofurantoin 24 h post seeding (described as immediate treatment), to simulate a preventative nitrofurantoin treatment. Alternatively, drug treatment occurred 48 h post seeding (described as delayed treatment) to simulate treating established emphysematous fibroblasts, such as what might be found in a more advanced case of emphysema. The supernatant of each treatment group was collected for analysis 3 days after nitrofurantoin application for the immediate treatment group (96 h after seeding) and 2 days after nitrofurantoin application for the delayed treatment group (96 h after seeding). This end point was chosen to allow cytokine expression (Fig. 3) and protein quantification by ECM ELISA (Fig. 7) to be measured at identical time points, as ECM ELISA requires a three-day incubation after treatment to detect a quantifiable difference in ECM protein abundance [34].

WI-38 (healthy) fibroblast IL-6 expression was not found to be significantly altered by the application of any nitrofurantoin concentration in the immediate or the delayed treatment groups. Mean IL-6 and IL-8 expression was not changed by nitrofurantoin treatment, and cytokine expression was found to be not statistically significant due to the wide variability in PHLF cytokine expression (Fig. 3).

The changes in cytokine expression after nitrofurantoin treatment were found to be neither significant, nor dose dependent, showing that nitrofurantoin treatment does not provoke an inflammatory response in lung fibroblasts.

3.2. Low concentration nitrofurantoin treatment increases fibroblast motility

Emphysematous fibroblast chemokinesis was examined over a 24 h time-lapse to investigate if nitrofurantoin treatment influenced the cellular migration speed of healthy and diseased fibroblasts. Migration is crucial to fibroblast maintenance of the lung ECM as the cells must frequently travel to sites of parenchymal damage through chemotaxis to commence ECM repair and maintenance [27,30]. Notably, increased motility is a strong indication of fibroblast activation and therefore, upregulated ECM repair [42,43]. The migration speed (μm/min) and mean squared displacement (MSD; μm^2) of both healthy and emphysematous fibroblasts were calculated from the tracked paths of individual fibroblasts over a 24 h time-lapse (Fig. 4).

The mean migration speed of the WI-38 (healthy) fibroblasts was not found to be significantly different to that of the untreated primary emphysematous fibroblasts (Fig. 4A). However, emphysematous fibroblasts treated with 2 μg/mL of nitrofurantoin (immediate treatment) displayed significantly increased migration speed compared to both WI-38 (2 μg/mL immediate treatment: 0.686 ± 0.02 μm/min vs. WI-38: 0.617 ± 0.02 μm/min; $p = 0.041$) and control emphysematous fibroblasts (0.613 ± 0.01 μm/min; $p = 0.0014$). This nitrofurantoin induced migration speed upregulation could suggest that the fibroblasts have entered an activated phenotype and are therefore primed to repair ECM damage. Although the (likely multifactorial [44]) molecular mechanisms used by nitrofurantoin to alter fibroblast activity remain poorly understood, nitrofurantoin treatment may activate signalling pathways that induce fibroblast activation, such as the TGF-β/SMAD or NF-κB pathways, thus stimulating ECM repair [45,46]. Notably, nitrofurantoin interacts with estrogen receptor α (ERα) [47], potentially stimulating oestrogen signalling pathway activity and thereby influencing the NF-κB pathway [48].

The mean migration speed of fibroblasts immediately treated with 10 μg/mL of nitrofurantoin was not significantly different from the control group (0.661 ± 0.02 μm/min vs. 0.613 ± 0.01 μm/min; $p = 0.242$) nor from the speed of fibroblasts immediately treated with 2 μg/mL (0.661 ± 0.02 μm/min vs. 0.686 ± 0.02 μm/min; $p = 0.91$). However, the mean migration speed of fibroblasts immediately treated with 20 μg/mL was significantly lower than that of the immediate 2 μg/mL treatment group (0.602 ± 0.02 μg/mL vs. 0.686 ± 0.02 μg/mL; $p = 0.0009$), indicating that the stimulatory effects of nitrofurantoin on fibroblast motility were not dose dependent. Furthermore, the mean squared displacement values calculated from the cell tracking (Fig. 4B) supports the findings of Fig. 4A, as the 2 μg/mL immediate nitrofurantoin treatment group was also found to have higher MSD compared to both the WI-38 fibroblasts and untreated emphysematous fibroblasts. Likewise, the MSD of the delayed nitrofurantoin treatment groups (Fig. 4C) supports the migration speed findings in Fig. 4A, as all delayed treatment groups displayed lower MSD than the healthy fibroblasts and untreated fibroblasts control group.

The reduction in migration speed after the immediate 20 μg/mL nitrofurantoin treatment could be related to the toxicity of the drug, as the concentration is approaching the upper limit of the toxicity curve (Fig. 2B). The proximity of the PHLF nitrofurantoin IC80 (19.6 ± 1.6 μg/mL) and the 20 μg/mL treatment groups concentration could indicate that the 20 μg/mL nitrofurantoin treatment caused reduced motility due to cellular stress. The toxicity of nitrofurantoin potentially reversed the upregulated migration seen in the 2 μg/mL treatment group and thus,

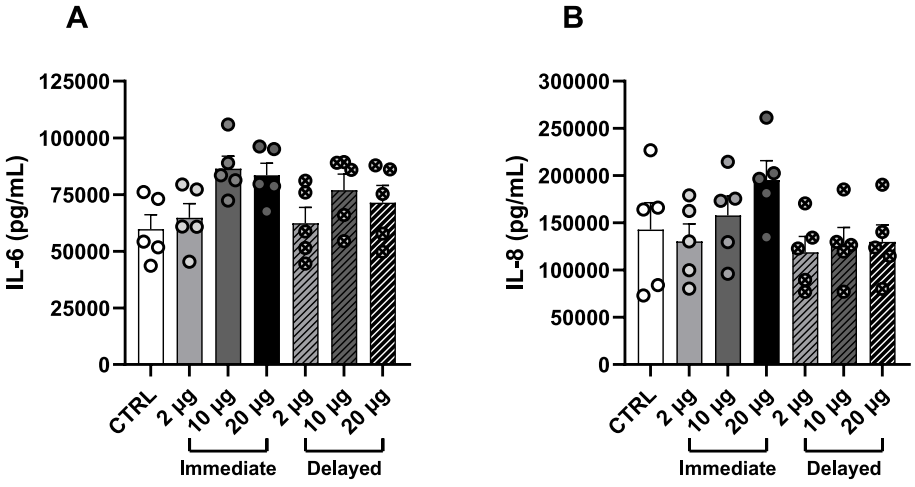

Fig. 3. Changes in (**A**) IL-6 & (**B**) IL-8 production by primary emphysematous fibroblasts when seeded on a coating of collagen-1 and treated with TNF-α, TGF-β and left untreated (CTRL) or treated with varying concentrations of nitrofurantoin. Data is represented as % change in IL-6/IL-8 expression with 100 % being the average IL-6/IL-8 expression of untreated (control) primary emphysematous fibroblasts. Data is displayed as mean ± SEM, $n = 5$ for all treatment groups with each cell line represented as a point. Statistical analysis was determined by one-way ANOVA with Tukey's multiple comparison post-test.

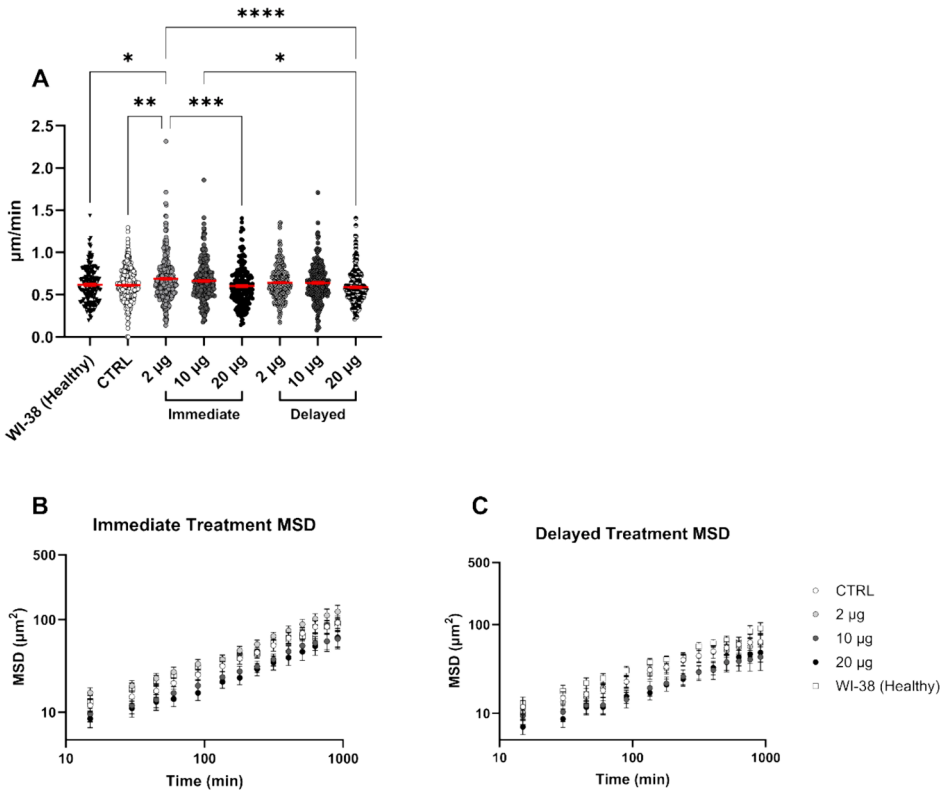

Fig. 4. Nitrofurantoin treatment raises the motility of primary emphysematous fibroblasts in a non-dose dependent manner. WI-38 and primary emphysematous cell lines were tracked over a 24 h period using phase-contrast microscopy after varying concentrations of nitrofurantoin treatment to examine changes in fibroblast motility. (**A**) Collated fibroblast migration speed (μm/min) is displayed as mean ± SEM (displayed as red bars), $n > 50$ for WI-38 cells and $n > 250$ for all primary cells (n > 50 from each cell line), (* $p < 0.05$, ** $p < 0.01$, *** $p < 0.001$, **** $p < 0.0001$). Statistical analysis was performed using one-way ANOVA with Tukey's multiple comparison post-test. The mean squared displacement (μm^2) of WI-38 and primary emphysematous cell lines was calculated from cell trajectories after a 24 h time-lapse (1440 min). Data is displayed as mean ± SEM, $n > 250$ for all treatment groups excluding CTRL (WI-38 cells) which had $n > 50$. (**B**) MSD of WI-38 and primary emphysematous cell lines when treated with nitrofurantoin 24 h after seeding (immediate treatment). (**C**) MSD of WI-38 and primary emphysematous cell lines when treated with nitrofurantoin 48 h after seeding (delayed treatment). (For interpretation of the references to colour in this figure legend, the reader is referred to the web version of this article.)

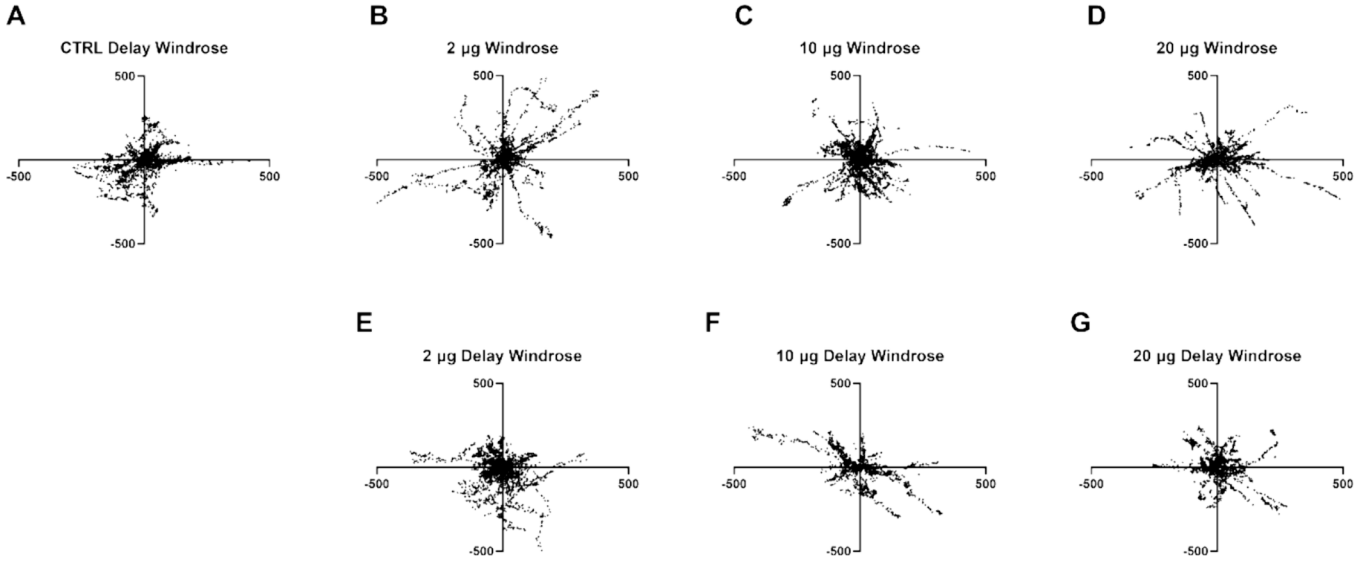

Fig. 5. Fibroblast displacement was raised after nitrofurantoin treatment. Windrose plots depicting the paths taken by emphysematous fibroblasts over a 24 h time-lapse normalised such that each path begins at the point (0,0 μm), $n > 50$. Fibroblasts were (**A**) left untreated, subjected to (**B**) 2 μg/mL, (**C**) 10 μg/mL, or (**D**) 20 μg/mL of nitrofurantoin. Additionally, the fibroblasts were also examined after delayed treatment using (**E**) 2 μg/mL, (**F**) 20 μg/mL or (**G**) 20 μg/mL of nitrofurantoin.

may have caused the effect to not be dose dependent. This drug toxicity suppressing fibroblast migration speed effect is also present in the 10 μg/mL treatment group, resulting in fibroblast migration speed that is neither significantly lower than the 2 μg/mL immediate treatment group, nor significantly higher than the untreated control group.

The influence of nitrofurantoin treatment on fibroblast motility was far less pronounced in the delayed treatment groups, as none were found to be significantly different from either the healthy control or the untreated emphysematous cells (Fig. 4A). The ineffectiveness of the delayed nitrofurantoin treatment could suggest that the influence of nitrofurantoin on cell motility had not yet taken effect. Notably, the delayed 20 μg/mL treatment group migration speed was significantly reduced compared to the 2 μg/mL immediate treatment group (0.590 ± 0.01 μm/min vs. 0.686 ± 0.02 μm/min; $p < 0.0001$). This significant decrease most likely suggests that although the migration speed of the delayed 2 μg/mL treatment group had not yet taken effect, the cytotoxicity of the delayed 20 μg/mL treatment group had reduced fibroblast migration speed. The altered migration speed of nitrofurantoin treated fibroblasts indicates that nitrofurantoin was most effective after immediate treatment, promoting migration when applied to fibroblasts at relatively low doses such as 2 μg/mL and. The increased migration speed of nitrofurantoin treated fibroblasts allows for more efficient ECM repair and could be caused by triggering an activated phenotype in fibroblasts [30].

The tracked paths taken by emphysematous cells were normalised to (0,0 μm) to visually demonstrate the impact of nitrofurantoin treatment on fibroblast motility via Wind-Rose plots (Fig. 5). Fig. 5A demonstrates that the paths taken by untreated emphysematous fibroblast cell lines appear to cluster around the point of origin (0,0 μm), whereas Fig. 5B-D show that fibroblasts appear to migrate farther from the site of origin after nitrofurantoin treatment. The Wind-Rose plots displaying the migration of fibroblasts after delayed treatment display similar migration to that of the untreated control cells (Fig. 5E, F).

The increase in fibroblast migration after nitrofurantoin treatment could suggest that fibroblasts are activated to begin ECM repair after 2 μg/mL nitrofurantoin treatment. Notably, fibroblasts that have entered a pro-ECM repair phenotype typically display alterations to their behaviour beyond increased motility such as increased proliferation and shifts in cellular morphology, as fibroblasts' actin cytoskeletons undergo conformational changes [43,49–51]. Cellular motility and morphology are closely linked as both are primarily governed by the actin cytoskeleton through conformational shifts that facilitate fibroblast functions such as migration or ECM deposition [52].

3.3. Nitrofurantoin treatment alters fibroblast morphology by increasing cell area and lowering roundness

The mean cell area (μm^2) and roundness of WI-38 and PHLF over a 24 h period was calculated to quantify changes in fibroblast morphology (Fig. 6A). The mean two-dimensional cell area of healthy fibroblasts was found to be significantly upregulated compared against untreated emphysematous cells (3590 ± 167.5 μm^2 vs. 2926 ± 75.7 μm^2; $p = 0.0045$), however, nitrofurantoin treatment was shown to significantly upregulate cell area in all treatment groups, excluding delayed 2 μg/mL treated fibroblasts (Fig. 6A). Fibroblast cell area did not respond to nitrofurantoin treatment in a dose dependent manner, as observed in the cell motility results (Fig. 5). However, unlike the non-dose dependent changes in migration speed, all fibroblasts displayed an approximately uniform increase in cell size (between 3518 ± 115.6 and 3863 ± 127.8 μm^2), except the delayed 2 μg/mL treated fibroblasts (3046 ± 89.7

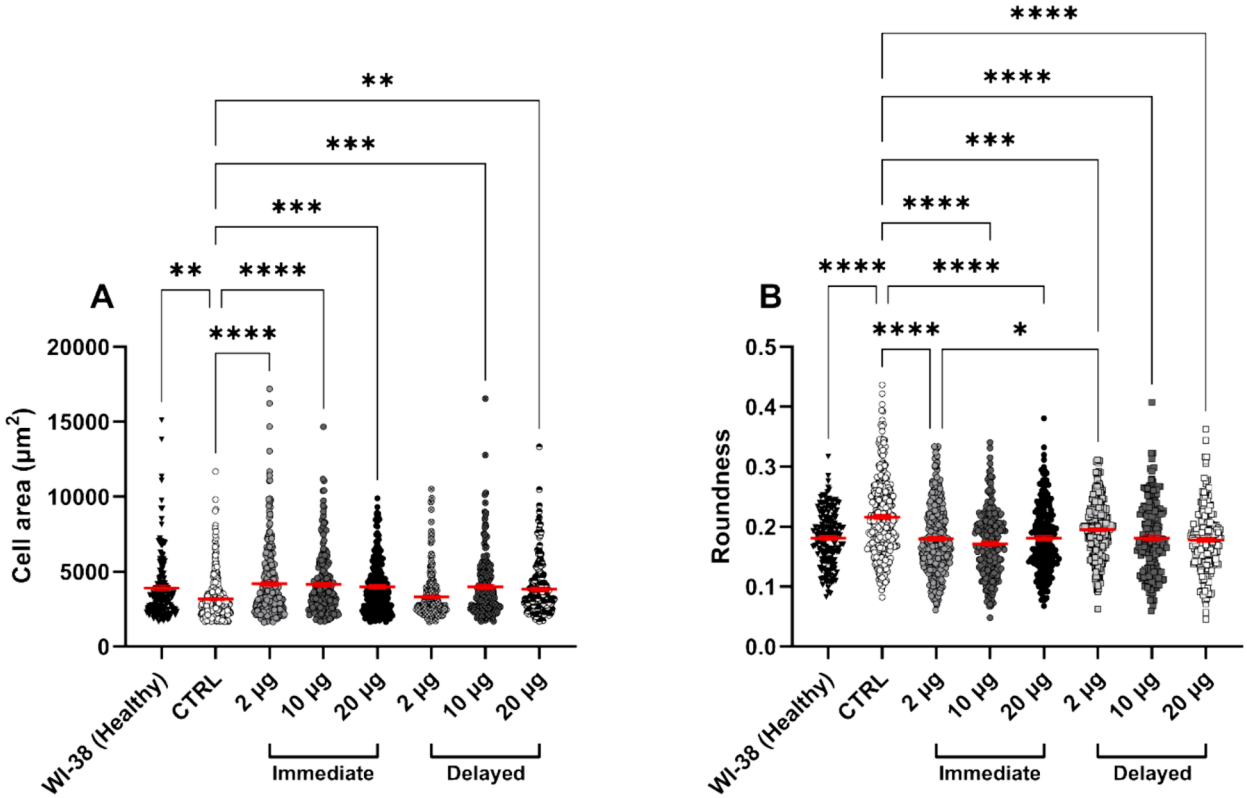

Fig. 6. Nitrofurantoin treatment alters fibroblast morphology by increasing cell area and decreasing roundness**.** Fibroblasts were tracked to determine the average 2-dimensional cell area and roundness of primary emphysematous fibroblasts over a 24 h time-lapse after nitrofurantoin treatment. (**A**) Mean cell area of fibroblasts was presented as mean ± SEM (displayed as red bars). (**B**) Mean roundness of fibroblasts was presented as mean ± SEM (displayed as red bars). $n > 50$ for WI-38 cells and $n > 250$ for all primary cells ($n > 50$ from each cell line), (* $p < 0.05$, ** $p < 0.01$, *** $p < 0.001$, **** $p < 0.0001$). Statistical analysis was performed using one-way ANOVA with Tukey's multiple comparison post-test. (For interpretation of the references to colour in this figure legend, the reader is referred to the web version of this article.)

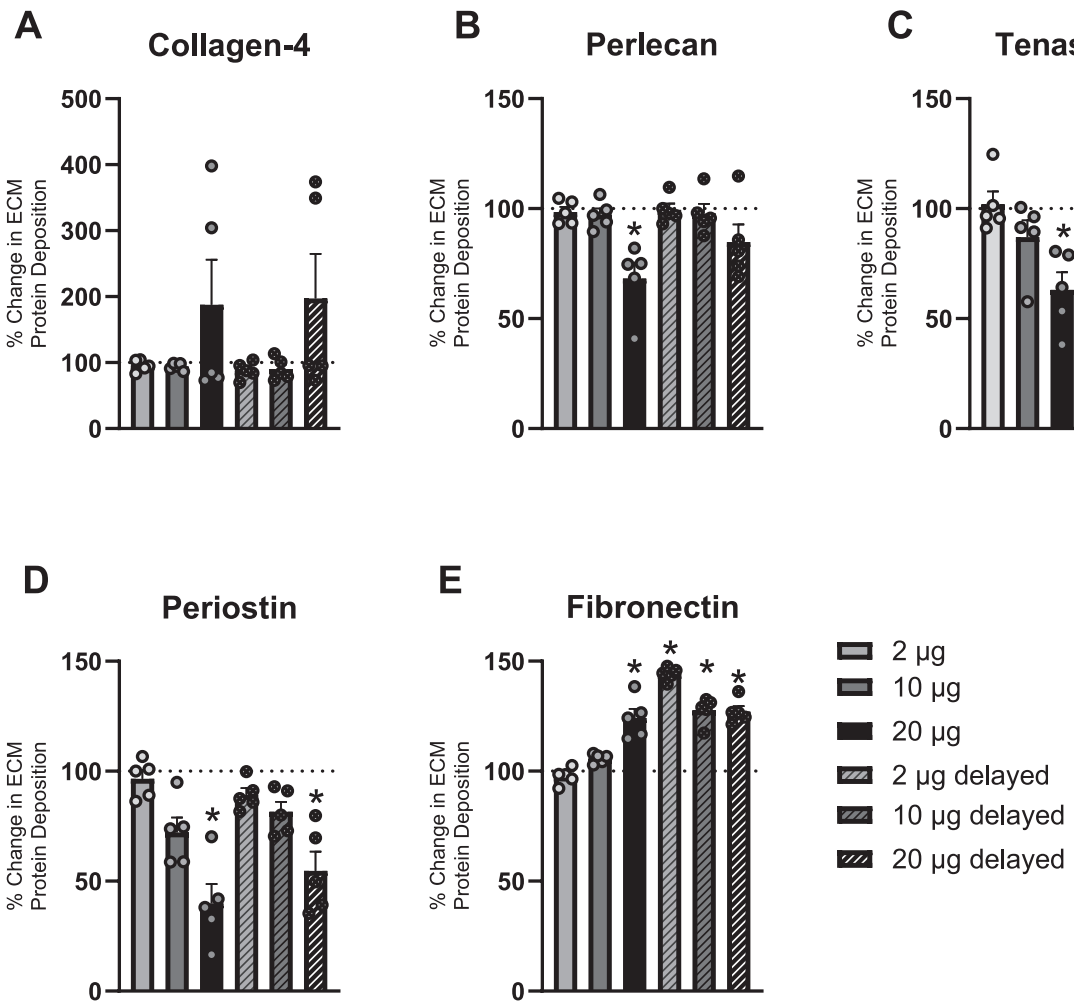

Fig. 7. Nitrofurantoin treatment reduced the expression of tenascin-C, periostin and perlecan while raising fibronectin expression. The percentage change in deposition of the ECM proteins (**A**) collagen-4, (**B**) perlecan, (**C**) fibronectin, (**D**) tenascin-C, (**E**) periostin by primary emphysematous fibroblasts after nitrofurantoin treatment. Data is represented as % change in ECM protein expression where 100 % represents the average protein expression of untreated primary emphysematous fibroblasts. Data is displayed as mean ± SEM, $n = 5$ for all treatments with each cell line represented as a point, * Indicates a treatment group is significantly different from control (100 % ECM protein expression; * $p < 0.05$). Statistical analysis was determined by one-way ANOVA with Tukey's multiple comparison post-test.

μm^2). Interestingly, the elevated cell size of nitrofurantoin treated emphysematous fibroblasts was comparable to the size of healthy cells, suggesting that the nitrofurantoin treatment could be correcting aspects of diseased fibroblast behaviour. The increase in cell size is potentially priming the diseased fibroblasts to behave similarly to healthy fibroblasts, or alternatively, the drug may induce a proto-myofibroblastic or myofibroblastic phenotype that upregulates ECM protein deposition [49]. A study by Uhal et al. [53] that divided fibroblasts into a small, medium, and large populations based on cell size found that medium size fibroblasts had the greatest percentage of cells in the synthesis (S) and gap 2 (G2) phases of the cell cycle, where the cell prepares for mitosis, and therefore the greatest proliferation. Furthermore, only the large fibroblast population displayed α-smooth muscle actin (α-SMA), a marker of myofibroblast differentiation/fibroblast activation [53]. This study indicates that the nitrofurantoin induced upregulation in cell size likely encourages proliferative and activated fibroblast phenotypes by increasing the proportion of fibroblasts that possess 'large' or 'medium' phenotypes. Additionally, the results of Fig. 4A did not align with the changes in cell migration seen in Fig. 6A, as the 20 µg/mL treatments failed to increase migration speed yet displayed the same increase in cell size as immediate 2 µg/mL or 10 µg/mL nitrofurantoin treatment. Although the cause of this discrepancy remains unclear, the differential response is potentially linked to cell size. For example, increased migration speed due to nitrofurantoin may only occur after cell size has increased, therefore the higher toxicity of the 20 µg/mL immediate and delayed treatments may have caused the increase in migration speed to be slowed due to cell stress. Furthermore, the increased migration speed of the 20 µg/mL treatment groups may become more apparent if given a longer incubation time.

Changes in fibroblast cell size due to nitrofurantoin treatment were mirrored in the fibroblast mean roundness (Fig. 6B) as WI-38 fibroblasts had significantly lower roundness when compared against untreated emphysematous fibroblasts (0.18 ± 0.004 vs. 0.22 ± 0.004; $p < 0.0001$). Furthermore, all fibroblasts treated with nitrofurantoin displayed significantly lower roundness compared to untreated diseased cells. As with cell size (Fig. 6A), the decreased mean roundness of nitrofurantoin treated cells resulted in diseased cells of comparable morphology to healthy fibroblasts, in terms of roundness. Interestingly, the immediate treatment 2 µg/mL fibroblasts and delayed treatment 2 µg/mL fibroblasts displayed a significant difference as the delayed treatment group displayed higher roundness than the standard treatment group (0.18 ± 0.003 vs. 0.20 ± 0.003; $p = 0.042$). This difference was likely due to the low dosage of the delayed 2 µg/mL treatment group requiring a longer incubation time to alter fibroblast roundness. As was observed in the motility and cell area results (Fig. 5A, 6A), no dose dependency was found in the mean roundness of nitrofurantoin treated

fibroblasts. A high roundness value alongside a lower cell area can be associated with a quiescent, deactivated fibroblast phenotype [54], therefore, the decreased roundness of fibroblasts after nitrofurantoin treatment supports the cell motility (Fig. 4A) results by further indicating that nitrofurantoin stimulates fibroblasts to enter an activated, potentially myofibroblastic phenotype. Notably, nitrofurantoin could exert a corrective effect on emphysematous fibroblasts morphology by restoring the cell size and roundness to that of a healthy fibroblast. Correcting fibroblast morphology indicates that the cellular cytoskeleton has been altered, potentially facilitating ECM repair by improving the ECM homeostatic capability of the diseased cells after treatment. Together, the changes to both cell two-dimensional area and roundness support the notion that the nitrofurantoin could be inducing an activated phenotype in emphysematous fibroblasts.

3.4. Emphysematous fibroblast ECM protein deposition largely unaffected by nitrofurantoin treatment

Relative ECM protein deposition was quantified using ECM ELISA 72 h after immediate nitrofurantoin application and 48 h after delayed nitrofurantoin application to examine the effect of treatment on emphysematous fibroblast ECM protein deposition. Cells were seeded on a collagen-1 coating to improve cell adherence and to promote fibroblast function [55], and additionally, all fibroblasts were stimulated with both TNF-α and TGF-β at 2 ng/mL to further induce ECM deposition. All data is displayed as the relative percentage change in ECM protein deposition compared against the ECM protein deposition of untreated diseased fibroblasts. The ECM proteins collagen-IV, perlecan, tenascin-C, periostin and fibronectin were selected for analysis as they perform a range of functions withing the lung ECM. For example, collagen-IV and fibronectin act as structural proteins, perlecan and periostin act as signalling proteins, whereas tenascin-C, fibronectin and periostin all influence dynamic cellular activity, such as adhesion and proliferation [56–59].

Collagen-IV deposition was found to be unaffected by nitrofurantoin treatment regardless of treatment group, despite the extreme variability in collagen-IV expression for the immediate and delayed 20 μg/mL treatment groups (Fig. 7A). The wide range of collagen-IV expression from the two 20 μg/mL treatment groups is most likely caused by the inherent variability of primary cells. Furthermore, nitrofurantoin treatment did not cause a significant difference in collagen-IV treatment when compared against the collagen-IV expression of untreated cells. Perlecan expression remained consistent regardless of nitrofurantoin dosage or treatment method (Fig. 7B), except for immediate 20 μg/mL nitrofurantoin treatment inducing a reduction in perlecan expression compared to untreated fibroblasts, potentially due to the cytotoxicity of nitrofurantoin at a concentration of 20 μg/mL. However, the 20 μg/mL delayed treatment group did not significantly lower the emphysematous fibroblast perlecan expression. Likewise, nitrofurantoin produced a similar pattern of tenascin-C expression as the ECM protein expression was unchanged by all treatment groups, excluding immediate 20 μg/mL treatment which was shown to significantly lower tenascin-C expression (Fig. 7C). Periostin expression was again similar to that of tenascin-C and perlecan, as all 2 and 10 μg/mL nitrofurantoin treatment groups did not significantly alter periostin production. However, both immediate and delayed 20 μg/mL nitrofurantoin treatment groups significantly reduced periostin expression (Fig. 7D).

Unlike other ECM proteins examined in this study, the expression of fibronectin was significantly increased by all delayed nitrofurantoin treatment groups and by the 20 μg/mL immediate treatment group (Fig. 7E). Fibronectin plays an essential role in wound repair and is a relatively ubiquitous protein throughout the body's ECM [60,61]. Notably, lung fibronectin volume is known to increase during emphysema, however, this only occurs in the small airways of the lung, whereas the parenchyma and large airways do not display altered ECM composition in terms of fibronectin [62]. The increase in fibronectin deposition is highly important to ECM repair as fibronectin is linked to the expression of pro-fibrotic genes that could further support ECM repair activity in fibroblasts [63]. The increased production of fibronectin may indicate that nitrofurantoin indirectly causes pulmonary fibrosis through fibroblast-fibronectin interactions that alter fibroblast dynamic cellular activity by upregulating ECM repair. Nitrofurantoin treatment was only found to alter ECM protein expressions when treated with 20 μg/mL, except for fibronectin.

The consistent pattern of significantly reductions in ECM protein deposition only after immediate or delayed 20 μg/mL nitrofurantoin treatment is most likely indicative of a reduction in ECM protein deposition due to cell stress caused by nitrofurantoin cytotoxicity. A reduction in cell viability due to the low nitrofurantoin IC80 of PHLF cells is more likely to have limited ECM protein production than a downregulation in ECM protein expression after nitrofurantoin treatment. Moreover, the unchanged collagen-IV, periostin, perlecan and tenascin-C expression raises further questions about the mechanism used by nitrofurantoin to cause lung fibrosis in patients, as fibroblasts in a fibrotic lung would be expected to have upregulated deposition of a range of ECM proteins. These ECM ELISA results differ from the migration and morphology findings (Figs. 4 and 6) that suggest nitrofurantoin treatment induces an activated fibroblast phenotype that consequently stimulates ECM repair; however, the ECM ELISA results did not show that nitrofurantoin treatment would alter ECM maintenance in the emphysematous lung. Nitrofurantoin induced lung fibrosis may require a longer nitrofurantoin incubation to be modelled, as lung fibrosis is typically found in patients that are taking the drug for extended periods of time as prophylactic [20,21]. Furthermore, nitrofurantoin induced pulmonary fibrosis may be the result of complex interactions between multiple lung cell populations, rather than just lung fibroblasts, and would therefore require more complex co-culture-based models of the lung to be replicated *in vitro*. Although the ECM ELISA performed for this study did not find an increase in collagen-IV, perlecan, periostin or tenascin-C production, nitrofurantoin may primarily upregulate the production of other ECM proteins such as fibronectin and others that were not examined in this study. Alternatively, nitrofurantoin could upregulate fibroblast organisation of the ECM by stimulating behaviours that raise ECM stiffness without altering ECM protein deposition, such as ECM protein crosslinking [64].

4. Conclusion

The results suggest that nitrofurantoin holds promise as an innovative treatment for emphysema; however, its potential is impeded by associated toxicity. Additionally, the mechanism through which nitrofurantoin promotes extracellular matrix (ECM) production in fibroblasts remains unclear, posing limitations to its therapeutic viability. While nitrofurantoin did not demonstrate an increase in overall ECM deposition (excluding fibronectin), it may enhance the organization of emphysematous ECM protein deposition by inducing an activated phenotype in lung fibroblasts. This activation could lead to improved ECM organization without necessarily upregulating ECM deposition, such as through ECM proteins cross-linking. The findings from this research indicate that low-dose nitrofurantoin could serve as a promising treatment for emphysema, provided that the drug's cytotoxic effects are mitigated, potentially through the exploration of innovative pharmaceutical formulation strategies. Additional investigations are necessary to explore the impact of a wider spectrum of nitrofurantoin concentrations, duration and dosing schedule on both *in vitro* and *in vivo* models to better understand the impact of nitrofurantoin on fibroblast viability and motility.

Ethical Statement

Primary human lung fibroblasts were extracted from the explanted or resected lung parenchyma of emphysema patients following resection

or lung transplantation. Written informed consent was obtained from each patient pre-operatively and the study was approved by the Human Ethic University of Sydney (10140) and the Central Sydney Area Health Service (approval code #X14-0045) on the 8th of April 2014.

CRediT authorship contribution statement

Mathew N. Leslie: . **Zara Sheikh:** Writing – review & editing, Writing – original draft, Visualization, Methodology, Investigation, Formal analysis, Data curation. **Dikaia Xenaki:** Writing – review & editing, Resources, Methodology, Investigation. **Brian G. Oliver:** Writing – review & editing, Resources, Methodology. **Paul M. Young:** Writing – review & editing, Resources, Conceptualization. **Daniela Traini:** Writing – review & editing, Writing – original draft, Validation, Supervision, Resources, Conceptualization. **Hui Xin Ong:** Writing – review & editing, Writing – original draft, Validation, Supervision, Resources, Methodology, Conceptualization.

Declaration of competing interest

The authors declare that they have no known competing financial interests or personal relationships that could have appeared to influence the work reported in this paper.

Acknowledgements

M.N.L. is the recipient of the Woolcock Emphysema Centre Scholarship with support from the Ernest Hein Family Foundation. Daniela Traini acknowledges the support provided by a Fellowship grant from the National Health and Medical Research Council (NHMRC) of Australia (APP1173363).

References

[1] Frantz C, Stewart KM, Weaver VM. The extracellular matrix at a glance. J Cell Sci 2010;123:4195–200. https://doi.org/10.1242/jcs.023820.
[2] Macklem PT. The mechanics of breathing. Am J Respir Crit Care Med 1998;157:S88–94. https://doi.org/10.1164/ajrccm.157.4.nhlbi-5.
[3] Burgstaller G, Oehrle B, Gerckens M, White ES, Schiller HB, Eickelberg O. The instructive extracellular matrix of the lung: basic composition and alterations in chronic lung disease. Eur Respir J 2017;50. https://doi.org/10.1183/13993003.01805-2016.
[4] Rohrer F. Physiologie der Atembewegung. In *Handbuch der Normalen und Pathologischen Physiologie: Zweiter Band Atmung; Aufnahme und Abgabe Gasförmiger Stoffe*, Bethe A, Embden Gv, Bergmann G, Ellinger A, Amersbach K, Bayer G, Brunner A, Felix W, Flury F, Geigel A, Heubner W, Hofbauer L, Liljestrand G, Renner O, Rohrer F, Sauerbruch F, Skramlik E, Staehelin R, Eds.; Springer: Berlin, Heidelberg; 1925. p. 70–127 ISBN 978-3-642-91002-9.
[5] Matsuda M, Fung YC, Sobin SS. Collagen and elastin fibers in human pulmonary alveolar mouths and ducts. J Appl Physiol 1987;63:1185–94. https://doi.org/10.1152/jappl.1987.63.3.1185.
[6] Holz O, Zühlke I, Jaksztat E, Müller KC, Welker L, Nakashima M, et al. Lung fibroblasts from patients with emphysema show a reduced proliferation rate in culture. Eur Respir J 2004;24:575–9. https://doi.org/10.1183/09031936.04.00143703.
[7] Tracy LE, Minasian RA, Caterson EJ. Extracellular matrix and dermal fibroblast function in the healing wound. Adv Wound Care (New Rochelle) 2016;5:119–36. https://doi.org/10.1089/wound.2014.0561.
[8] Humphrey JD, Dufresne ER, Schwartz MA. Mechanotransduction and extracellular matrix homeostasis. Nat Rev Mol Cell Biol 2014;15:802–12. https://doi.org/10.1038/nrm3896.
[9] Leung DY, Glagov S, Mathews MB. Cyclic stretching stimulates synthesis of matrix components by arterial smooth muscle cells in vitro. Science 1976;191:475–7. https://doi.org/10.1126/science.128820.
[10] Faffe DS, Zin WA. Lung parenchymal mechanics in health and disease. Physiol Rev 2009;89:759–75. https://doi.org/10.1152/physrev.00019.2007.
[11] Suki B, Stamenovic D, Hubmayr R. Lung parenchymal mechanics. Compr Physiol 2011;1:1317. https://doi.org/10.1002/cphy.c100033.
[12] Wang J-H-C, Thampatty BP. An introductory review of cell mechanobiology. Biomech Model Mechanobiol 2006;5:1–16. https://doi.org/10.1007/s10237-005-0012-z.
[13] Decramer M, Janssens W, Miravitlles M. Chronic Obstructive pulmonary disease. Lancet 2012;379:1341–51. https://doi.org/10.1016/S0140-6736(11)60968-9.
[14] Goldklang M, Stockley R. Pathophysiology of emphysema and implications. Chronic Obstr Pulm Dis 2016;3:454–8. https://doi.org/10.15326/jcopdf.3.1.2015.0175.
[15] Bates JHT, Davis GS, Majumdar A, Butnor KJ, Suki B. Linking parenchymal disease progression to changes in lung mechanical function by percolation. Am J Respir Crit Care Med 2007;176:617–23. https://doi.org/10.1164/rccm.200611-1739OC.
[16] O'Donnell DE, Laveneziana P. Physiology and consequences of lung hyperinflation in COPD. Eur Respir Rev 2006;15:61–7. https://doi.org/10.1183/09059180.00010002.
[17] Leslie MN, Chou J, Young PM, Traini D, Bradbury P, Ong HX. How do mechanics guide fibroblast activity? Complex disruptions during emphysema shape cellular responses and limit research. Bioengineering 2021;8:110. https://doi.org/10.3390/bioengineering8080110.
[18] Suki B, Sato S, Parameswaran H, Szabari MV, Takahashi A, Bartolák-Suki E. Emphysema and mechanical stress-induced lung remodeling. Physiology 2013;28:404–13. https://doi.org/10.1152/physiol.00041.2013.
[19] Ghazvini H, Taheri K, Edalati E, Sedighi M, Mirkalantari S. Virulence factors and antimicrobial resistance in uropathogenic escherichia coli strains isolated from cystitis and pyelonephritis. Turk J Med Sci 2019;49:361–7. https://doi.org/10.3906/sag-1805-100.
[20] Prakash UBS. Pulmonary reaction to nitrofurantoin. Semin Respirat Med 1980;2:70–5. https://doi.org/10.1055/s-2007-1012142.
[21] Naureen S, Faruqi S, Hart S, Jawad N, Kennan N. Nitrofurantoin induced pulmonary fibrosis: a case series. Eur Respir J 2021;58. https://doi.org/10.1183/13993003.congress-2021.PA2374.
[22] Celli BR, MacNee W. ATS/ERS task force standards for the diagnosis and treatment of patients with Copd: a summary of the ATS/ERS position paper. Eur Respir J 2004;23:932–46. https://doi.org/10.1183/09031936.04.00014304.
[23] Stringer C, Wang T, Michaelos M, Pachitariu M. Cellpose: a generalist algorithm for cellular segmentation. Nat Methods 2021;18:100–6. https://doi.org/10.1038/s41592-020-01018-x.
[24] Pachitariu M, Stringer C. Cellpose 2.0: how to train your own model. Nat Methods 2022;19:1634–41. https://doi.org/10.1038/s41592-022-01663-4.
[25] Aragaki H, Ogoh K, Kondo Y, Aoki K. LIM tracker: a software package for cell tracking and analysis with advanced interactivity. Sci Rep 2022;12:2702. https://doi.org/10.1038/s41598-022-06269-6.
[26] Sethi S, Murphy TF. Infection in the pathogenesis and course of chronic obstructive pulmonary diseasecurrent concepts. N Engl J Med 2008;359:2355–65. https://doi.org.ezproxy.library.sydney.edu.au/10.1056/NEJMra0800353.
[27] Raghow R. The role of extracellular matrix in postinflammatory wound healing and fibrosis. FASEB J 1994;8:823–31. https://doi.org/10.1096/fasebj.8.11.8070631.
[28] Akhmetshina A, Palumbo K, Dees C, Bergmann C, Venalis P, Zerr P, et al. Activation of canonical wnt signalling is required for TGF-β-mediated fibrosis. Nat Commun 2012;3:735. https://doi.org/10.1038/ncomms1734.
[29] Hinz B. The extracellular matrix and transforming growth factor-B1: tale of a strained relationship. Matrix Biol 2015;47:54–65. https://doi.org/10.1016/j.matbio.2015.05.006.
[30] Postlethwaite AE, Seyer JM. Stimulation of fibroblast chemotaxis by human recombinant tumor necrosis factor alpha (TNF-alpha) and a synthetic TNF-alpha 31–68 peptide. J Exp Med 1990;172:1749–56. https://doi.org/10.1084/jem.172.6.1749.
[31] Chiang C-H, Chuang C-H, Liu S-L. Transforming growth factor-B1 and tumor necrosis factor-α are associated with clinical severity and airflow limitation of COPD in an additive manner. Lung 2014;192:95–102. https://doi.org/10.1007/s00408-013-9520-2.
[32] Sorkun MC, Khetan A, Er S. AqSolDB, a curated reference set of aqueous solubility and 2D descriptors for a diverse set of compounds. Sci Data 2019;6:143. https://doi.org/10.1038/s41597-019-0151-1.
[33] Michiels C, Remacle J. Quantitative study of natural antioxidant systems for cellular nitrofurantoin toxicity. Biochim Biophys Acta 1988;967:341–7. https://doi.org/10.1016/0304-4165(88)90096-7.
[34] Leslie MN, Marasini N, Sheikh Z, Young PM, Traini D, Ong HX. Development of inhalable spray dried nitrofurantoin formulations for the treatment of emphysema. Pharmaceutics 2022;15:146. https://doi.org/10.3390/pharmaceutics15010146.
[35] Schwaiblmair M, Behr W, Haeckel T, Märkl B, Foerg W, Berghaus T. Drug induced interstitial lung disease. Open Respir Med J 2012;6:63–74. https://doi.org/10.2174/1874306401206010063.
[36] Brandao-Rangel MAR, Oliveira CR, da Silva Olímpio FR, Aimbire F, Mateus-Silva JR, Chaluppe FA, et al. Hydrolyzed collagen induces an anti-inflammatory response that induces proliferation of skin fibroblast and keratinocytes. Nutrients 2022;14:4975. https://doi.org/10.3390/nu14234975.
[37] Prudente R, Ferrari R, Mesquita C, Machado L, Franco E, Godoy I, et al. Nine-year follow-up of interleukin 6 in chronic obstructive pulmonary disease – complementary results from previous studies. Int J Chron Obstruct Pulmon Dis 2021;16:3019–26. https://doi.org/10.2147/COPD.S328266.
[38] Hussein FGM, Mohammed RS, Khattab RA, Al-Sharawy LA. Serum interleukin-6 in chronic obstructive pulmonary disease patients and its relation to severity and acute exacerbation. Egypt J Bronchol. 2022;16:10. https://doi.org/10.1186/s43168-022-00115-z.
[39] Hackett T-L, Vriesde NRTF, AL-Fouadi M, Mostaco-Guidolin L, Maftoun D, Hsieh A, Coxson N et al. The role of the dynamic lung extracellular matrix environment on fibroblast morphology and inflammation. Cells 2022;11:185. doi:10.3390/cells11020185.
[40] Long X, Ye Y, Zhang L, Liu P, Yu W, Wei F, et al. IL-8, a novel messenger to cross-link inflammation and tumor EMT via autocrine and paracrine pathways (review). Int J Oncol 2016;48:5–12. https://doi.org/10.3892/ijo.2015.3234.
[41] Cesta MC, Zippoli M, Marsiglia C, Gavioli EM, Mantelli F, Allegretti M, et al. The role of interleukin-8 in lung inflammation and injury: implications for the

management of COVID-19 and hyperinflammatory acute respiratory distress syndrome. Front Pharmacol 2022;12.
[42] Hinz B. Formation and function of the myofibroblast during tissue repair. J Invest Dermatol 2007;127:526–37. https://doi.org/10.1038/sj.jid.5700613.
[43] Woodley JP, Lambert DW, Asencio IO. Understanding fibroblast behavior in 3D biomaterials. Tissue Eng Part B Rev 2022;28:569–78. https://doi.org/10.1089/ten.TEB.2021.0010.
[44] Gardiner BJ, Stewardson AJ, Abbott IJ, Peleg AY. Nitrofurantoin and fosfomycin for resistant urinary tract infections: old drugs for emerging problems. Aust Prescr 2019;42. https://doi.org/10.18773/austprescr.2019.002.
[45] Grande MT, López-Novoa JM. Fibroblast activation and myofibroblast generation in obstructive nephropathy. Nat Rev Nephrol 2009;5:319–28. https://doi.org/10.1038/nrneph.2009.74.
[46] Htwe SS, Harrington H, Knox A, Rose F, Aylott J, Haycock JW, et al. Investigating NF-κB signaling in lung fibroblasts in 2D and 3D culture systems. Respir Res 2015;16:144. https://doi.org/10.1186/s12931-015-0302-7.
[47] Sipes NS, Martin MT, Kothiya P, Reif DM, Judson RS, Richard AM, et al. Profiling 976 ToxCast chemicals across 331 enzymatic and receptor signaling assays. Chem Res Toxicol 2013;26:878–95. https://doi.org/10.1021/tx400021f.
[48] Frasor J, El-Shennawy L, Stender JD, Kastrati I. NFκB affects Estrogen receptor expression and activity in breast cancer through multiple mechanisms. Mol Cell Endocrinol 2015;418:235–9. https://doi.org/10.1016/j.mce.2014.09.013.
[49] D'Urso M, Kurniawan NA. Mechanical and physical regulation of fibroblast-myofibroblast transition: from cellular mechanoresponse to tissue pathology. Front Bioeng Biotechnol 2020;8. https://doi.org/10.3389/fbioe.2020.609653.
[50] Qin Z, Fisher GJ, Voorhees JJ, Quan T. Actin cytoskeleton assembly regulates collagen production via TGF-β Type II Receptor in human skin fibroblasts. J Cell Mol Med 2018;22:4085–96. https://doi.org/10.1111/jcmm.13685.
[51] Vasilopoulos Y, Gkretsi V, Armaka M, Aidinis V, Kollias G. Actin cytoskeleton dynamics linked to synovial fibroblast activation as a novel pathogenic principle in TNF-driven arthritis. iii23–iii28 Ann Rheum Dis 2007;66. https://doi.org/10.1136/ard.2007.079822.
[52] Kole TP, Tseng Y, Jiang I, Katz JL, Wirtz D. Intracellular mechanics of migrating fibroblasts. Mol Biol Cell 2005;16:328–38. https://doi.org/10.1091/mbc.E04-06-0485.
[53] Uhal BD, Ramos C, Joshi I, Bifero A, Pardo A, Selman M. Cell size, cell cycle, and α-smooth muscle actin expression by primary human lung fibroblasts. Am J Physiol-Lung Cell Mol Physiol 1998;275:L998–1005. https://doi.org/10.1152/ajplung.1998.275.5.L998.
[54] Svystonyuk DA, Ngu JM, Mewhort HE, Lipon BD, Teng G, Guzzardi DG, et al. Fibroblast growth factor-2 regulates human cardiac myofibroblast-mediated extracellular matrix remodeling. J Transl Med 2015;13:147. https://doi.org/10.1186/s12967-015-0510-4.
[55] Li W, Fan J, Chen M, Guan S, Sawcer D, Bokoch GM, et al. Mechanism of human dermal fibroblast migration driven by type I collagen and platelet-derived growth factor-BB. MBoC 2004;15:294–309. https://doi.org/10.1091/mbc.e03-05-0352.
[56] Parisi L, Toffoli A, Ghezzi B, Mozzoni B, Lumetti S, Macaluso GM. A Glance on the Role of fibronectin in controlling cell response at biomaterial interface. Jpn Dent Sci Rev 2020;56:50–5. https://doi.org/10.1016/j.jdsr.2019.11.002.
[57] Yue B. Biology of the extracellular matrix: an overview. J Glaucoma 2014:S20–3. https://doi.org/10.1097/IJG.0000000000000108.
[58] Chiquet M, Gelman L, Lutz R, Maier S. From mechanotransduction to extracellular matrix gene expression in fibroblasts. Biochimica et Biophysica Acta (BBA) - Molecular Cell Res 2009;1793:911–20. https://doi.org/10.1016/j.bbamcr.2009.01.012.
[59] Okamoto M, Hoshino T, Kitasato Y, Sakazaki Y, Kawayama T, Fujimoto K, et al. Periostin, a matrix protein, is a novel biomarker for idiopathic interstitial pneumonias. Eur Respir J 2011;37:1119–27. https://doi.org/10.1183/09031936.00059810.
[60] Lenselink EA. Role of fibronectin in normal wound healing. Int Wound J 2013;12:313–6. https://doi.org/10.1111/iwj.12109.
[61] Mao Y, Schwarzbauer JE. Fibronectin fibrillogenesis, a cell-mediated matrix assembly process. Matrix Biol 2005;24:389–99. https://doi.org/10.1016/j.matbio.2005.06.008.
[62] Hackett T-L, Vriesde NRTF, AL-Fouadi M, Mostaco-Guidolin L, Maftoun D, Hsieh A, et al. The role of the dynamic lung extracellular matrix environment on fibroblast morphology and inflammation. Cells 2022;11:185, doi:10.3390/cells11020185.
[63] Maddali P, Ambesi A, McKeown-Longo PJ. Induction of pro-inflammatory genes by fibronectin DAMPs in three fibroblast cell lines: role of TAK1 and MAP kinases. PLoS One 2023;18:e0286390.
[64] Semkova ME, Hsuan JJ. TGFβ-1 induced cross-linking of the extracellular matrix of primary human dermal fibroblasts. Int J Mol Sci 2021;22:984. https://doi.org/10.3390/ijms22030984.